Effect of the surface morphology of solidified droplet on remelting between neighboring aluminum droplets

Hao Yi[1,2], Lehua Qi[1,2,*], Jun Luo[1,2,*], Daicong Zhang[1,2], Hejun Li[3] and Xianghui Hou[4]

1. School of Mechanical Engineering, Northwestern Polytechnical University, Xi'an 710072, China

2. The Key Laboratory of Contemporary Design and Integrated Manufacturing Technology, Ministry of Education, Xi'an 710072, China

3. School of Materials Science and Engineering, Northwestern Polytechnical University, Xi'an 710072, China

4. Faculty of Engineering, University of Nottingham, Nottingham NG7 2RD, United Kingdom

First author's E-mail address: yihao19881116@gmail. com (H. Yi) or yihao@mail.nwpu.edu.cn (H. Yi).

* Corresponding author: qilehua@nwpu.edu.cn (L. Qi); luojun@nwpu.edu.cn (J. Luo) .

Abstract:

Good metallurgical bonding between neighboring droplets is essential in droplet-based 3D printing. However, although the mechanism of remelting has clearly been mastered, cold laps are still common internal defects of formed parts in uniform aluminum droplets deposition manufacturing, which is due to the overlook of the surface morphologies of solidified droplets. Here, for the first time, the blocking effect of ripples and solidification angles on the fusion between droplets is revealed. To investigate the detailed process of remelting, a 3D numerical model was developed, basing on the volume of fluid (VOF) method. Experiments and simulations show that the remelting process between neighboring droplets can be divided into two stages according to the transient contact between the second droplet and the substrate. In the first stage, a non-intuitive result is observed that cold laps can also be formed even if the remelting conditions are satisfied in theory. Ripples on the surface of previously-deposited droplet block its direct contact with the new-coming droplet. In the second stage, cold laps on bottom surface are formed due to incomplete filling of liquid metal when the solidification angle is greater than 90°. Furthermore, these cold laps are difficult to be completely avoided by improving the temperature parameters. To address this problem, a novel strategy of decreasing the thermal conductivity coefficient of the substrate is proposed. This method effectively promotes remelting between droplets by eliminating ripples and decreasing solidification angles.

Keywords: 3D printing; aluminum droplets; metallurgical bonding; ripples; solidification angle.

1. Introduction

Droplet-based 3D printing is a kind of novel direct-write techniques [1, 2], and it is considered to be a promising method for numerous applications, such as printing of flexible circuits [3, 4], advanced electronic components [5, 6] and metal parts [7]. In the manufacturing processes, uniform metal micro-droplets as the basic building blocks are sequentially deposited onto a programmable substrate to fabricate complex 3D parts from their CAD models. However, due to the high temperature gradient and large surface tension of molten aluminum alloys, it is still a huge challenge to directly print high-quality structures from molten aluminum droplets.

Fusion behavior at the droplet/droplet interface is a fundamental issue in printing 3D metal structures. Poor remelting between neighboring droplets will lead to defects, such as cold lap pores, which result in the decrease of metallurgical bonding [8]. To determine the critical conditions of remelting, a calculated model of the interfacial temperature between neighboring droplets was developed [9]. The thermal behaviors of single droplet [10, 11] and multi -droplets [12] sequentially impacting on substrates were investigated by experimental and numerical studies. The proper temperature parameters for achieving good metallurgical bonding between neighboring droplets were then ascertained [13]. Moreover, the scanning steps were optimized to decrease the inner porosities of the formed parts in droplet-based 3D printing [14]. However, the performance has not been significantly improved, cold lap pores are still common internal defects of the formed parts in aluminum droplets 3D printing. Therefore, other influencing factors in remelting have to be considered.

A number of theoretical and experimental studies [15-18] on molten metal droplets impact suggest that some ripples will be formed on the droplet surface after the complete solidification of the droplet. The reason of this phenomenon is that the solidification of metal droplets is always accompanied with underdamped oscillation, which is subsequently “frozen” by phase change to become ripples with different scales. Furthermore, because the surface tension of molten aluminum droplet is relatively large and the solidification process is rapid, the solidification angles of the deposition aluminum droplets are usually larger than 90° [16, 19, 20]. These facts bring us to the question that whether these surface morphologies influence the remelting behavior between neighboring droplets in 3D printing. However, this interesting case has yet to be well studied.

The present work aims to investigate the effect of surface morphologies of solidified droplets on the remelting behavior between neighboring droplets during the horizontal deposition process. To this end, some droplet deposition experiments were conducted, and a 3D numerical model was also developed, basing on the VOF method. By comparing the experimental and simulation results, the remelting process between two neighboring droplets is divided into two stages according to the transient contact between the second droplet and the substrate. The influencing mechanism of surface morphologies, including ripples and solidification angles, was then revealed by experiments and simulations. Finally, a method of using a substrate with relatively lower thermal conductivity was proposed. The corresponding experimental results verify that this proposed method can effectively promote the remelting between neighboring droplets by eliminating ripples and decreasing solidification angles.

2. Experimental and numerical approach

2.1 Experimental approach

As shown in Fig. 1(a), the uniform aluminum droplet deposition manufacturing system mainly consists of a uniform metal droplet generator, a droplet deposition subsystem and a hypoxic condition control subsystem. In short, this system works as follows. First, the metal blank was grinded to remove its oxide skin and then melted in a graphite crucible. A vibration bar was driven by a specified waveform which was created by a pulse generator. Under the periodical vibration of the ceramic bar, the liquid metal was forced out of a nozzle to generate uniform molten metal droplets. During the ejection process, the piezoelectric actuator was placed in a cooling case, and the liquid metal could maintain filling the cavity in the crucible under the back pressure. The droplet deposition subsystem consisted of a programmable multi-axes controller (PMAC), a substrate and a 3D programmable platform. The motion of the platform was controlled according to the computer numerical control (CNC) file generated by model design and slice software process. As shown in Fig. 1(b), under the cooperative control of droplet ejection and platform movement, the metal droplets were sequentially deposited and fused together to fabricate 3D structures. The temperatures of molten metal droplets and substrate were measured and controlled by heater controllers. During the uniform droplet deposition process, the metal droplet generator and the 3D platform were both enclosed in an argon gas environment. The oxygen and water vapor content of the argon gas

environment was kept below 1 PPM (parts per million) to prevent the molten aluminum droplets from being oxidized. The above subsystems were coordinately manipulated by an industrial personal computer (IPC) to complete the fabrication of complex shapes.

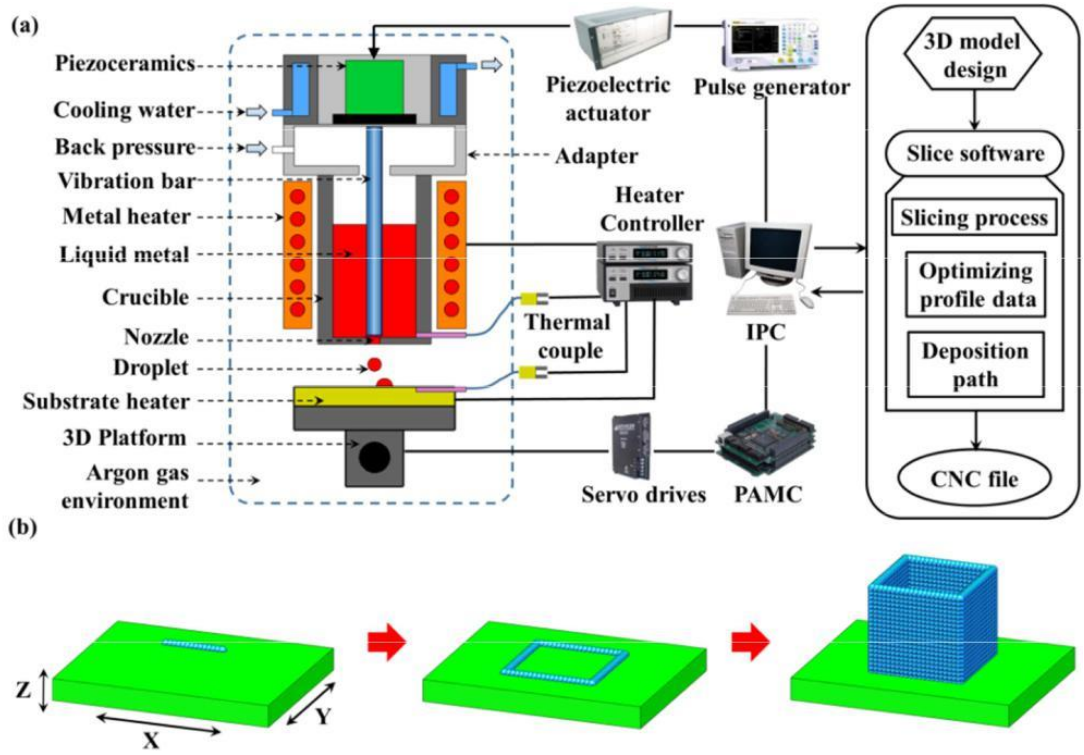

Fig. 1. Schematic diagram of (a) experimental setup and (b) process principle of uniform aluminum droplet deposition manufacturing.

In the deposition experiments, two 99.999% aluminum rods with the dimension of 35 mm× Φ20 mm were put into the graphite crucible and heated to a preset temperature. Uniform droplets were ejected out at a rate of 1-10Hz through a nozzle of ~450 μm in diameter. The perpendicular distance between the substrate and the nozzle was ~10 mm. H59 brass and one kind of silver-plated ceramic (which are commonly used in advanced electronics) were chosen as the materials of the substrate. 99.998% Argon gas was supplied to maintain an inert atmosphere to eliminate the oxidation of the molten aluminum droplets during the deposition process. The micro-morphologies of the deposition samples were obtained by using a scanning electron microscope (VEGA3-TESCAN).

2.2 Numerical approach

To analyze the detailed fluid flow and thermal behavior during the aluminum droplets horizontal deposition process, a 3D simulation model was developed, basing on the VOF method.

The mathematical principle of this simulation model is similar to the previous research [20, 21]. As shown in Fig. 2, the model mainly consists of two aluminum droplets and a substrate. The flow field of the molten droplet was solved by 3D Navier-Stokes, continuity and energy equations.

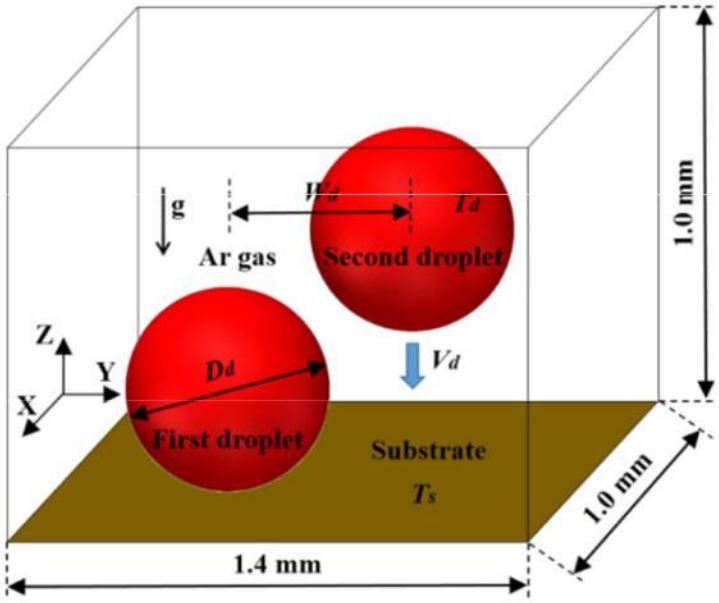

Fig. 2. Schematic diagram of the numerical model of two droplets successively depositing on the substrate.

In the uniform aluminum micro-droplet deposition manufacturing, the heat convection was less than 10% of the total energy of the molten droplets [15]. As a result, the heat dissipation of droplets during flying in the gas environment could be ignored [16]. After the impact, the heat transfer of molten aluminum droplet mainly depends on the heat conduction [17, 18, 20]. Therefore, the radiant heat transfer could also be ignored in this numerical modeling.

Pure aluminum was chosen for the present numerical modeling and experiment. To satisfy the precision of the numerical model, a minimum temperature range of 1K was given for the phase change of the pure aluminum droplet [20, 21]. The contact thermal resistance between the droplets and the substrate was set as $10^{-6}m^2KW^{-1}$ [22–24]. The pressure and velocity of the void region were set as zero. The boundary conditions of the computational domain and the substrate surface were set as ‘‘continuative’’ and “wall”, respective ly [20, 21]. The static contact angle between the droplet and the substrate was set as 90° [20, 21] . The physical properties of the pure aluminum are shown in Table 1 [25]. The initial conditions of the numerical model are shown in Table 2.

Table 1 Properties of pure aluminum used in the simulation and experiment

Properties	Value
Density ($kg \cdot m^{-3}$)	$\rho = 2368$
Dynamics viscosity ($Pa \cdot s$)	$\mu = 1.257 \times 10^{-3}$
Surface tension coefficient ($N \cdot m^{-1}$)	$\sigma = 0.868$
Heat conductivity coefficient ($W \cdot m^{-1} \cdot K^{-1}$)	$k_s = 220$
	$k_l = 96.4$
Specific heat capacity ($J \cdot kg^{-1} \cdot K^{-1}$)	$C_s = 1135$
	$C_l = 1086$
Latent heat for solidification ($J \cdot kg^{-1}$)	$L = 397\,500$
Liquidus temperature (K)	$T_l = 934$
Solidus temperature (K)	$T_s = 933$
Static contact angle (°)	$\theta = 90$

s = Solid; l = Liquid.

Table 2 Initial conditions of the numerical model.

Items	Value
Diameter of droplets D_d (μm)	500
Initial falling velocity of droplets v_d ($m \cdot s^{-1}$)	0.8
Deposition distance H (mm)	10
Initial temperatures of droplets T_d (K)	1223 1423 1623
Substrate temperature T_{sub} (K)	300 523 723
Scanning step W_d (μm)	400

A commercial software FlOW-3D 11.0.4 was used to implement the numerical model developed above. FLOW-3D provides a subroutine for the production of droplets. All parameters, such as the offset distance, dimensions, velocity, position and temperature can be set in this subroutine [26]. The code uses a finite volume/finite difference method to solve the Navier–Stokes equations for fluid flow. Equations were iteratively solved by using a minimum time step of 10^{-9} s. The computational grid consisted of about two million rectangular elements, equaling about 40 units per droplet diameter.

2.3 Experimental validation of the numerical model

Figure 3 shows the experimental and numerical results of two typically deposited neighboring droplets. The initial temperature of the droplet was 1223K, the substrate temperature was 523K, and

the scanning step was 400 μm. The experimental and simulation results show good agreement from the top, side and bottom views.

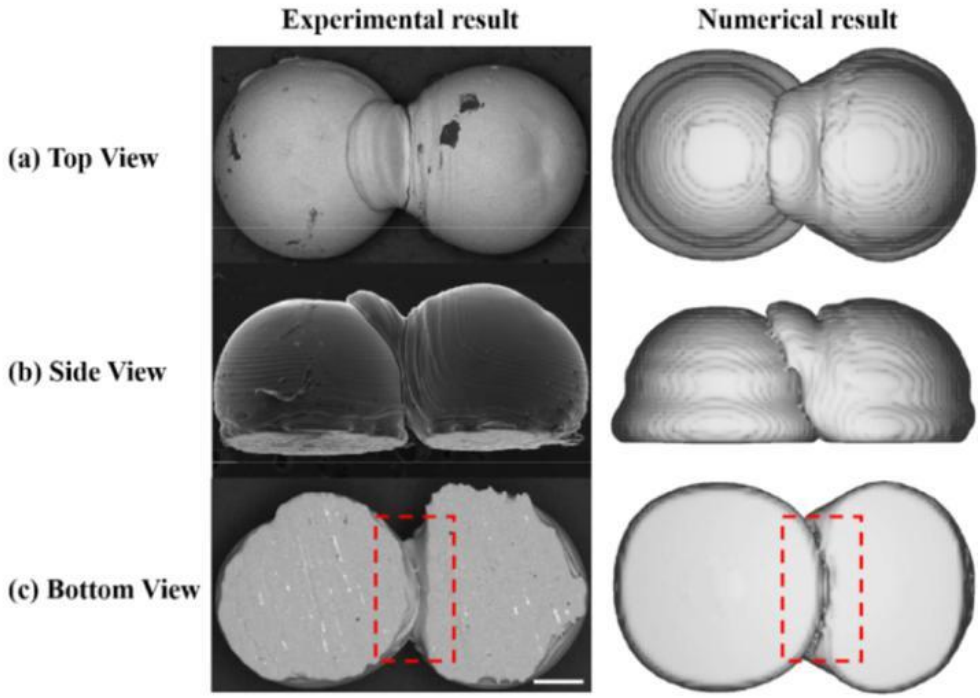

Fig. 3. Comparison of SEM photographs and simulation results of two neighboring aluminum droplets from (a) top view, (b) side view and (c) bottom view. The scale bar is 100 μm.

3. Results and discussion

3.1 Stage division of remelting process between neighboring droplets

To investigate the remelting process in depth, it is necessary to obtain a comprehensive understanding of the dynamic behavior during two neighboring droplets successive deposition. Figure 4 illustrates some characteristic snapshots of two neighboring droplets successive deposition, which consists of a few processes: (a) Two droplets begin to contact at point A; (b) The second droplet flows downwards along the first droplet and begins to contact with the substrate at point B. At this moment, a closed pore is temporarily formed between the two droplets and the substrate; (c) The second droplet continues to spread along the substrate while some portion of the molten metal fill in the temporary pore formed in process (b). However, the local solidification within the bottom area of the second droplet will lead to insufficient filling, and a cold lap pore will be eventually formed on the bottom surface of the two adjacent droplets; (d)-(e) Before the full solidification of

the second droplet, the residual liquid metal will oscillate up and down several times in the oblique direction to the substrate; (f) The second droplet is fully solidified.

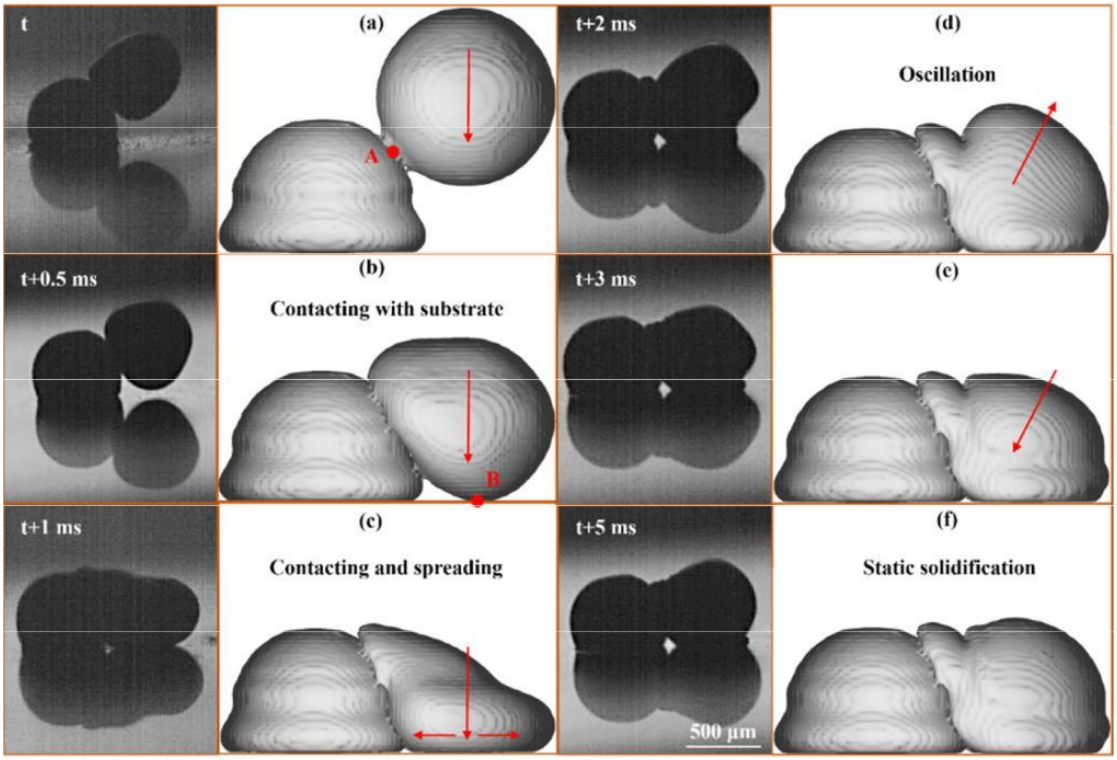

Fig. 4. Experimental and simulation images of shape evolution during two neighboring droplets successively impacting at (a) t, (b) t+0.5 ms, (c) t+1 ms, (d) t+2 ms, (e) t+3 ms and (f) t+5 ms.

The dynamics of droplet deposition depend on the value of Weber number (*We*) and Ohnesorge number (*Oh*), which can be calculated by Eq. (1) and Eq. (2):

$$We = \frac{\rho v_d^2 D_d}{\sigma} \quad (1)$$

$$Oh = \frac{\mu}{\sqrt{\rho \sigma D_d}} \quad (2)$$

The *We* number and *Oh* number in the experiment and simulation are about 0.88 and 1.24×10^{-3}, respectively. According to Schiaffino and Sonin [15], in this study, the droplet deposition is driven by the dynamic pressure of impacting. The dynamic spreading and oscillation are the results of the conversion interplay between kinetic and free surface energies. During above process (d) to (e), the second droplet keeps alternate spreading and recoiling in order to balance the kinetic energy and the surface energy. The oscillation of the second droplet will stop when its kinetic energy is fully dissipated by viscosity and solidification.

Comparing with the actual droplet deposition dynamic images, which were captured by a high-speed CCD, and the simulation results, it is concluded that the simulation results agree well with the experiments. Both results show that at first the two droplet contact, the second droplet then flows downwards along the first droplet. Next, the molten metal fill in the bottom void until the bottom area of the second droplet is fully solidified. At last, a cold lap pore will be formed (the bright spot between the two droplets and the substrate in Fig. 4). The shape of this pore will not be changed with the following oscillation of the second droplet. Time *t* corresponds to the instant of contact between the two neighboring droplets, and the whole freezing time of the second droplet is approximately 5 ms. Therefore, the remelting process between neighboring droplets can be divided into two different stages according to the transient contact between the second droplet and the substrate. In the first stage, there is no contact between the second droplet and the substrate. The main surface morphology influencing remelting behavior is the ripples on the first droplet surface. In the second stage, the second droplet begins to contact with the substrate. The residual liquid metal within the bottom region will fill in the pore temporarily formed between the two neighboring droplets and the substrate. The main surface morphology influencing remelting behavior is the solidification angle of the first droplet.

3.2 Blocking effect of ripples on the remelting between droplets

To achieve good remelting between neighboring droplets, the temperatures of the droplet and the substrate need to meet proper conditions. It is necessary to introduce a concept of the interfacial temperature of two contacting droplets. According to a previous report [27], the interfacial temperature T_i can be calculated as:

$$T_i = T_{surf} + (T_d - T_{surf})\left[1 - \exp\left(\frac{\alpha_s t}{R_c^2 k_s^2}\right) erfc\left(\frac{\sqrt{\alpha_s t}}{R_c k_s}\right)\right] \quad (3)$$

where T_{surf}, α_s, t and R_c are the surface temperature of the previously-deposited droplet, the thermal diffusivity of the droplet, the heat transfer time and the interfacial contact resistance, respectively.

The remelting behavior depends on the relation between the interfacial temperature T_i and the melting point T_m of the droplet. If $T_i > T_m$, remelting occurs in the contact region of the two neighboring droplets and vice versa.

First, the thermal gradient inside the droplet can be neglected, since the ratio of conduction heat transfer resistance within the droplet to the convective heat transfer resistance, which is quantified by the Biot number B_i, is below 0.015 in all the cases considered in this work. ($Bi=h_dD_d/k_d$ with the convection heat transfer coefficient h_d and the thermal conductivity of the new-coming droplet kd). T_{surf} was measured to be ~800K when the substrate temperature and deposition frequency were 523K and 10 Hz, respectively. The characteristic scales for t and R_c are~100 μs and $\sim 10^{-6} m^2 K W^{-1}$, respectively [27,28]. As a result, the interfacial temperature T_i is calculated to be ~940K which is above the melting point of aluminum. This implies that the interface between two neighboring droplets will be immediately remelted upon contact.

Figure 5 shows the experimental results under the conditions of T_d=1223K, T_{sub} =523K and f =10 Hz. According to the above analysis, remelting should occur between the neighboring droplets. However, a non-intuitive result is observed that there exists a poor remelting within the interface of two neighboring droplets. As shown in Fig. 5(c), it is clear that the two neighboring droplets only fuse at the peak of the ripples. From the fracture morphology in Fig. 5(d), it is found that the second droplet copies the ripples appearance on the first droplet. Moreover, as shown in Fig. 5(e), it can be found that the boundary between two neighboring droplets is clearly visible in some places at their interface, which indicates that cold laps are formed. Whereas, in some other places, the interface between them disappears, which shows the evidence of local remelting and fusing of the droplets. Closer examination of the cross-section of two successively-deposited droplets in Fig. 5(f) draws our attention to the alternating occurrence of cold lap and remelting.

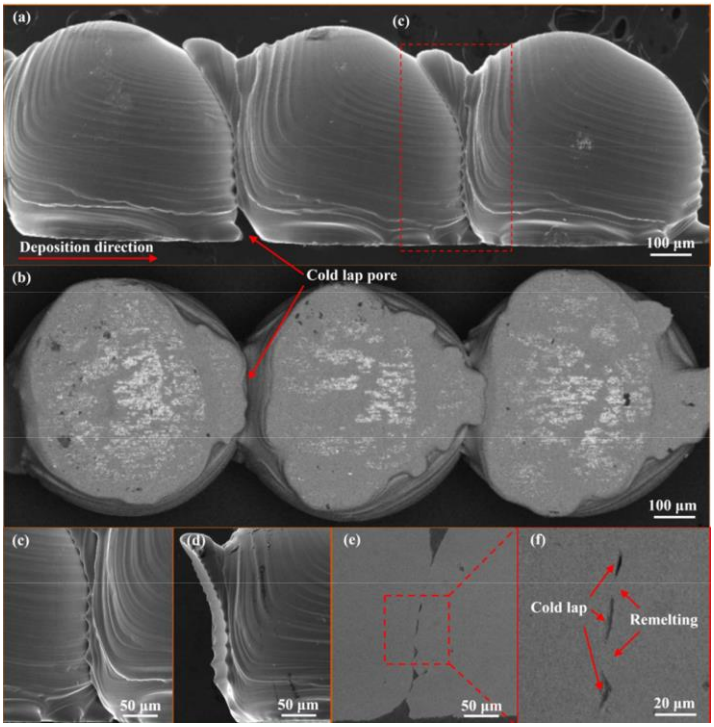

Fig. 5. SEM observation of (a) side view and (b) bottom view of successive deposition of aluminum droplets; (c) enlarged side view of the section of the printed metal trace in (a); (d) fracture of two neighboring droplets; (e) cross-section of two droplets successive deposition; (f) enlarged view of the selected section in (e).

To understand Fig. 5(c)–(f), it is helpful to turn to the numerical simulation results shown in Fig. 6 which were conducted under the same process parameters as the experiments in Fig. 5. Figure 6(a) shows the shape evolution and solid fraction distribution in Y-Z middle cross-section of two neighboring droplets. Time t=0 μs corresponds to the instant of contact between the two neighboring droplets. It is found that the remelting depth is relatively shallow (~10 μm) and the duration of that the second droplet flows down along the first droplet is relatively short (~400 μs). Under such conditions, the remelting depth is insufficient to melt all the ripples on the first droplet. As shown in Fig. 7, a simplified model is adapted to characterize the surface ripples of the previously-deposited droplet. When the remelting depth y_r is less than the ripple characteristic height h, the residual liquid in the second droplet will continue to fill in the void between the ripples driven by capillary pressure P_c. However, due to the existence of ambient gas, the back pressure P_g from the trapped gas will hinder the filling process of the residual liquid metal. When $P_c = P_g$, the filling process stops. As a result, the liquid metal penetration depth y_p is always less than (h-y_r). In other words, the residual liquid of the second droplet cannot completely fill the void between neighboring ripples on the first droplet. In the end, cold lap pores (highlighted by a red dotted box in Fig. 6(a)) are formed within

the ripple regions when the two metal droplets are completely solidified. Moreover, during the oblique impact of two neighboring droplets, the surrounding gas within the liquid-solid interface is strongly squeezed which leads to a pressure buildup in the gas under the new-coming droplet. The enhanced pressure results in a local dimple formation in the new-coming droplet, at the same time, the viscous shear stresses of the compressed gas increases quickly that decreases the escaping velocity of compressed gas. After impact, the trapped gas forms a bubble on the interface [29]. Ripples on the surface of previously-deposited droplet increase the chances of gas entrapment. Because the gas entrapment is the physical nature of droplet impact, it can be hardly avoided by changing the process parameters. Therefore, internal defects may also occur even if the remelting depth is further increased.

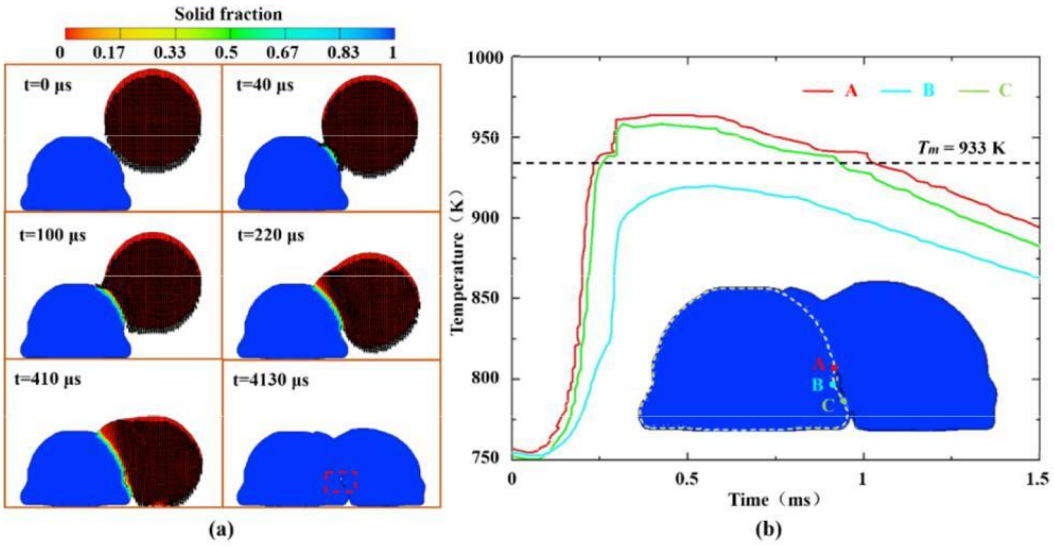

Fig. 6. Simulation results of (a) shape evolution and solid fraction distribution in Y- Z middle cross-section of two successively-deposited droplets; (b) temperature variation with time at three points (labeled A-C) on the surface of the first droplet during the deposition of the second droplet.

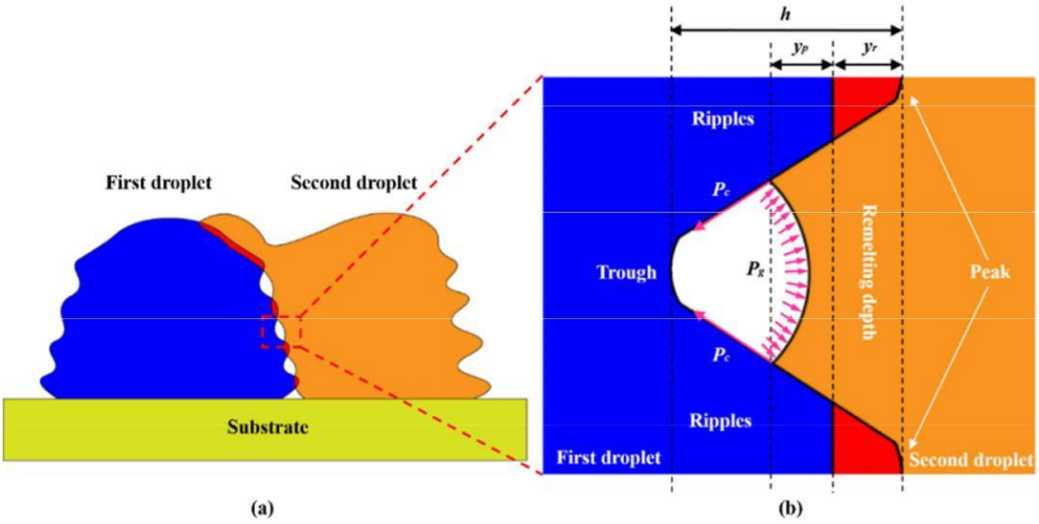

Fig. 7. Schematic of (a) two neighboring droplets depositing on substrate; (b) Simplified surface ripples model.

Figure 6(b) shows the temperature variation with time at three different points (labeled A-C) on the surface of the first droplet during the deposition of the second droplet. These three points of A, B and C correspond to the peak, trough and peak of two adjacent ripples respectively. Because the lapping and spreading process of the new-coming droplet is accompanied with heat dissipation, the temperature of the three points of A, B and C should be successively decreasing. However, a non-intuitive result is observed that the temperature of point A is the highest, followed by point C and point B. Moreover, the temperatures of point A and C both exceed the melting point of aluminum, while the temperature of point B is always below the melting point. The simulation results mean that remelting only occurs at point A and C. The time scale for remelting is ~100 μs, and this result is similar to the previous work conducted by Amon [28]. This numerical output is consistent with the experiments in Fig. 5, and the mechanism of the experimental phenomenon in Fig. 5 can be well explained. Due to the existence of surface ripples, the new-coming droplet cannot directly contact with the previously-deposited droplet. As the result of above force analysis, it can be drawn that the residual liquid metal cannot fill in the void within the ripples. Therefore, cold lap and remelting alternately appear on the interface of two neighboring droplets.

3.3 Blocking effect of solidification angle on the remelting between droplets

As clearly indicated in Fig. 3(c) and Fig. 5(b), a slender pore is formed on the bottom surface of two neighboring droplets. This result (dimension and location) is highly reproducible under

similar experimental conditions. Through a closer examination of the side view of the droplet bottom region in Fig. 3(b), Fig. 4 and Fig. 5(a), it can be found that the solidification angle of the previously-deposited droplet is larger than 90°. Th is surface morphology near the bottom region of the previously-deposited droplet will block its direct contact with the new-coming droplet. To achieve a good remelting within the bottom region, the pore needs to be filled in by the flow of residual liquid metal after the second droplet contacts with the substrate.

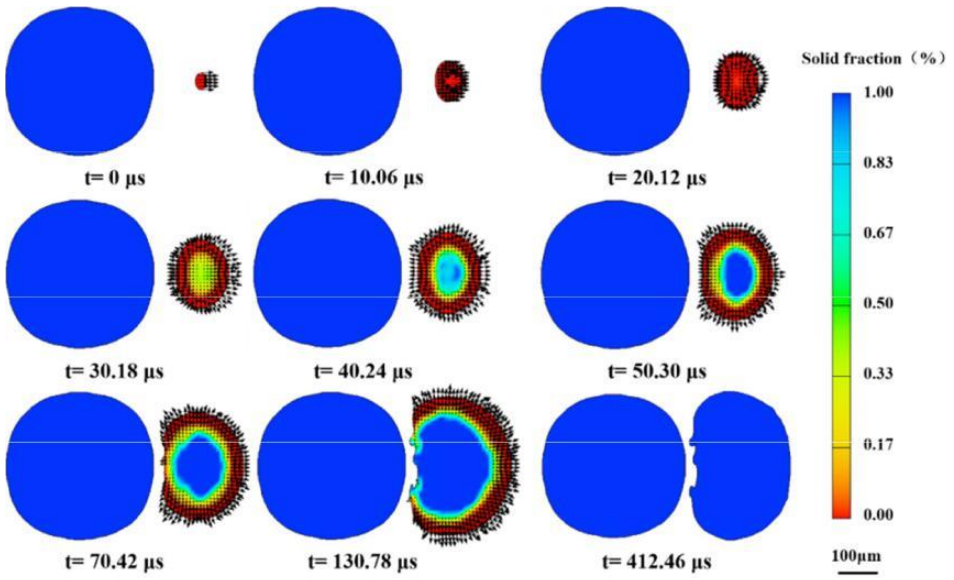

Fig. 8. Simulation results of shape evolution and solid fraction distribution in the X -Y bottom cross-section of two neighboring droplets.

Figure 8 shows the shape evolution and solid fraction distribution in X-Y bottom cross-section of two successively-deposited droplets. The black arrows represent the directions of local liquid flow. Time t =0 μs is defined as the instant time when the second droplet contacts with the substrate. According to the simulation results, when the second droplet begins to spread along the substrate, its velocity distribution on the bottom surface faces away from the first droplet. At t =20.12 μs, the second droplet symmetrically spreads along the substrate with respect to the initial impacting point, and the local solidification occurs at the same time. At t =40.24 μs, because of the local solidification within the bottom region and the resistance from the first droplet, the velocity component of the second droplet towards the first droplet starts to decrease. At t =70.42 μs, the velocity of liquid flow filling into the pore almost decreases to zero. Therefore, the shape of this bottom cold lap pore

remains unchanged. In other words, the filling time of liquid metal flow is about 50.30 μs. At t =412.46 μs, the bottom layer is solidified completely and a cold lap pore is formed on the bottom surface due to the incomplete filling.

Usually, the most sufficient way of eliminate cold lap is to increase the temperatures of the droplet and the substrate. Increasing the temperature parameters can increase the remelting depth and the filling time of liquid metal flow. To impart a measure of generality, the melt superheat dimensional parameter β [15], which characterizes the temperature differences between T_d, T_{sub} and T_m, is introduced.

$$\beta = \frac{T_d - T_m}{T_m - T_{sub}} \qquad (4)$$

Figure 9(a) shows the simulation results of solidification angle variation with β. Figure 9(b) shows the final shape variation with β in Y-Z cross-section and X-Y cross-section. It can be drawn that the solidification angle tends to decrease with the increase of β. Moreover, with the increase of β, the cold lap pore on the bottom surface tends to decrease until it completely disappears. However, on one side, even though the solidification angle has a decreasing tendency, it is always larger than 90°. On another side, in actual experiments, the phenomenon of excessive remelting occurred when the temperature of droplet and substrate were 1223K and 723K, respectively. The two neighboring droplets almost merged together, and the substrate was also remelted to a certain extent at the same time. The deposited droplets were difficult to be removed from the substrate, and this was undesirable in the uniform aluminum droplet deposition manufacture.

The reason for this experimental phenomenon can be explained by thermal energy analysis. At the transient moment of droplet impact, the thermal losses caused by heat conduction and convection can be ignored. As a result, the metal droplet impact process is assumed to be isothermal. Under such conditions, the thermal energy from the cooling of the new-coming droplet from T_d to T_m (before solidification) is:

$$E_{qd} = V_d \rho C_l (T_d - T_m) \qquad (5)$$

where V_d is the droplet volume. In this process, the remelted volume of the previously-deposited droplet is:

$$V_x = \frac{E_{qd}}{\rho C_s (T_m - T_{surf}) + \rho L} \qquad (6)$$

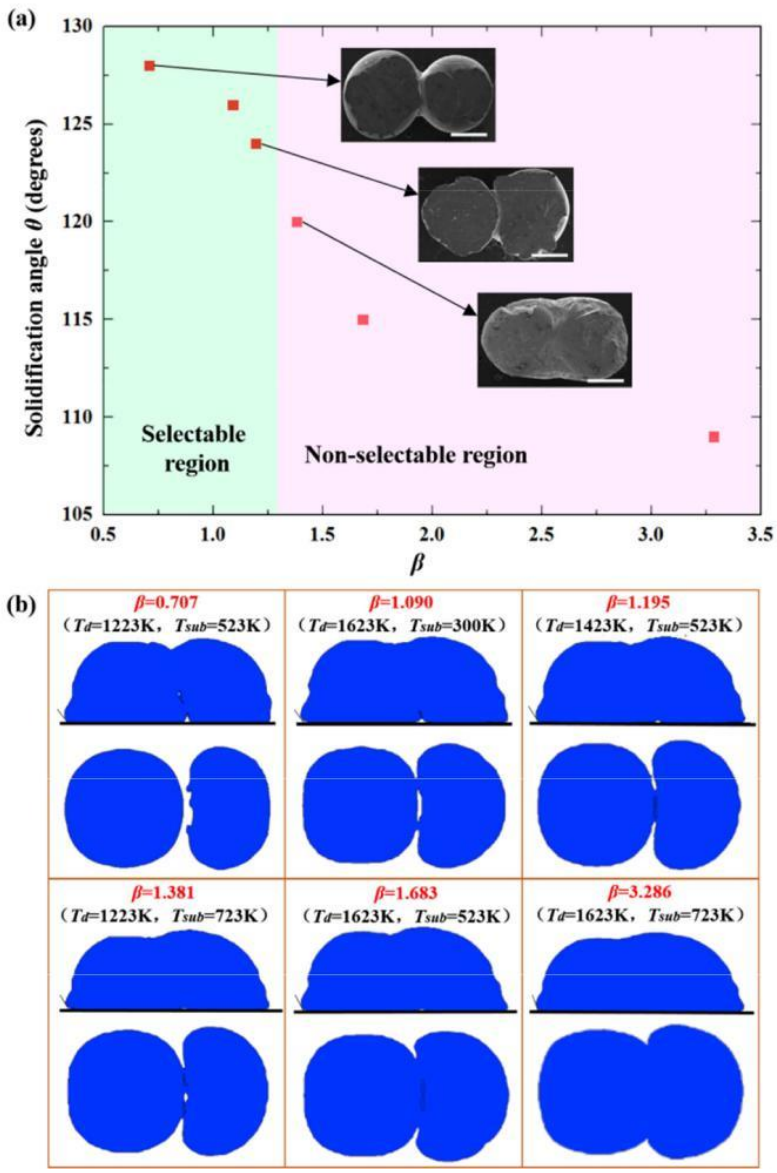

Fig. 9. Simulation results of (a) solidification angle and (b) final shape in Y-Z middle cross-section and X-Y cross-section variation with the melt superheat dimensional parameter β. The scale bar is 300 μm.

Under the conditions of T_d=1223K, T_{sub}=723K, f=10 Hz, T_{surf} was measured to be ~900K. Therefore, the volume fraction of the remelting section is calculated to be ~70%, which means that the two neighboring droplets are almost liquid state in the early stage of contacting. The neighboring droplets trend to accumulate under the drive of surface tension [30]. Therefore, it can be concluded that excessive remelting will occur before the cold lap pores on the bottom surface are eliminated by improving the temperature parameters.

3.4 A strategy to eliminate ripples and decrease solidification angles

Through the above discussion, it is suggested that ripples are adverse to the remelting between neighboring metal droplets. These surface ripples will block the direct contact between the second droplet and the first one. Furthermore, when the solidification angle is greater than 90°, cold lap pores will be formed on the bottom surface of deposited droplets due to the insufficient filling of residual liquid metal. The experimental and simulation results show that these cold laps can be hardly avoided by improving the temperatures of droplet and substrate. Therefore, it is very important to find a way to eliminate ripples and decrease the solidification angles of the droplets.

Besides the droplet temperature and substrate temperature, the thermal conductivity of the substrate is another important influencing factor of the remelting behavior between metal droplets. Figure 10 shows the simulation results of surface morphology of deposited droplet variation with the decrease of thermal conductivity of the substrate. It is found that the surface of the droplet tends to be smooth with the decrease of thermal conductivity of the substrate. When the substrate thermal conductivity is decreased from 400 W/(m·K) to 100 W/(m·K), the solidification angle of the deposition droplet decreases from an obtuse angle to an acute angle. The main reason for this phenomenon is that the solidification time of the droplet is prolonged with the decrease of thermal conductivity of the substrate. The liquid metal droplets rest in the equilibrium state throughout the process of solidification. As a result, the ripples will not be formed on the surface of the droplets. At the same time, the deposited droplets can reach a better spread.

One kind of silver-plated ceramic substrate was chosen to deposit the droplets. Here, the Ag coating was used to eliminate the bounce of metal droplets [31]. The thermal conductivity of this silver-plated ceramic substrate is ~100 W/(m·K). Comparing the experiment and the corresponding simulation in Fig. 10, it is concluded that the surface morphology of the deposition droplet in experiment agrees well with the simulation. Figure 11 shows the experimental results which were conducted with the similar temperature parameters (T_d=1223K, T_{sub} =523K, T_{surf} ~800K when f=1Hz) as Fig. 5. The only difference is the substrate thermal conductivity. It can be found that cold lap pores on the bottom surface can be effectively eliminated and the good fusion can also be achieved by decreasing the thermal conductivity of the substrate.

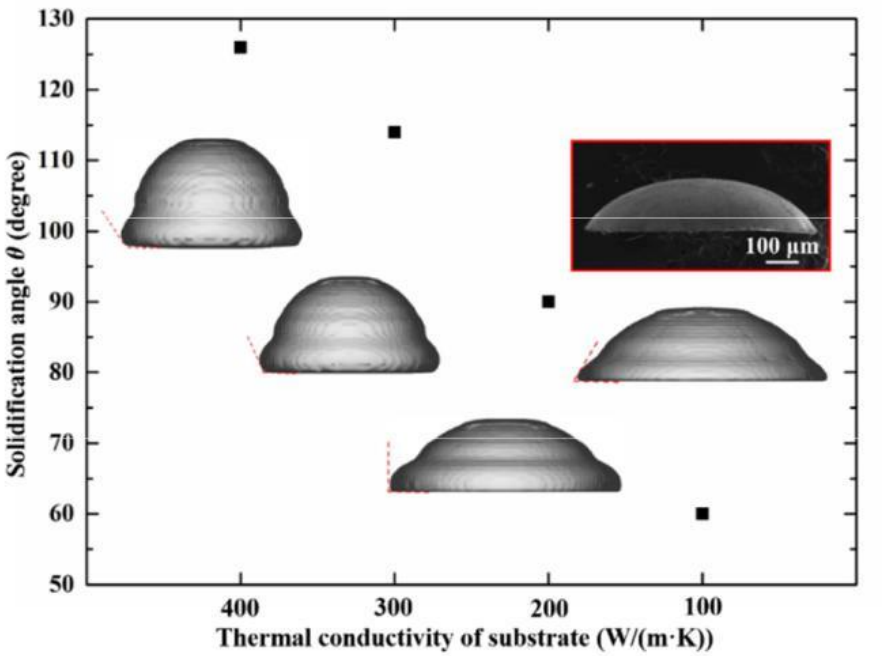

Fig. 10. Simulation results of surface morphology variation with the decrease of the thermal conductivity of the substrate and the SEM image of side view of the deposited droplet with the substrate thermal conductivity of ~100 W/(m·K).

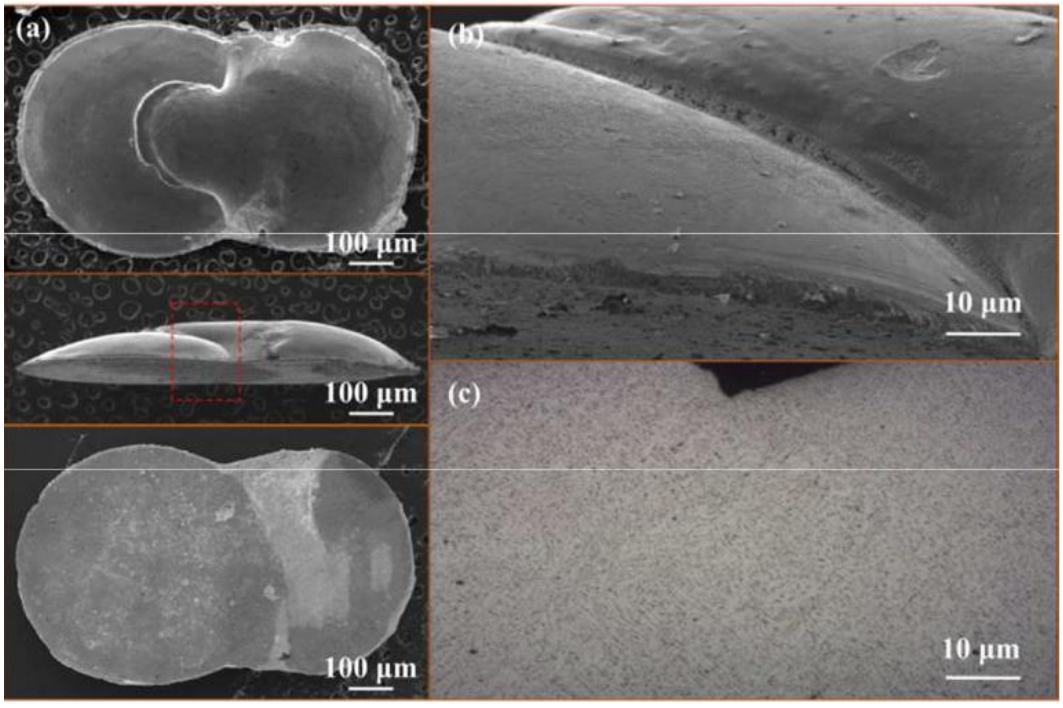

Fig. 11. SEM images of the morphology of (a) two neighboring droplets with the similar temperature parameters as those in Fig. 5; (b) enlarged side view of the selected section of the deposited metal trace in (a); (c) cross-section of the interface region in (a).

4. Conclusions

For the first time, the obstructive effect of surface morphologies, including ripples and solidification angles, on the remelting process between neighboring droplets is revealed. To investigate the detailed process during remelting between neighboring droplets, a 3D model was developed basing on the VOF method. The simulated morphology of deposited droplets agrees well with the experiments.

The remelting process between neighboring droplets can be divided into two stages according to the transient contact between the second droplet and the substrate. In the first stage, a non-intuitive result is observed that cold laps can also be formed even if the remelting conditions are satisfied in theory. This is mainly because ripples on the surface of the previously-deposited droplet will block its direct contact with the new-coming droplet. In the second stage, cold laps will be formed on the bottom surface due to the incomplete filling of residual liquid phase when the solidification angle is greater than 90°. These cold lap pores are difficult to be completely avoided if the issues of surface morphologies are not addressed.

Finally, a novel strategy of eliminating ripples and decreasing solidification angles to promote remelting is proposed. Through experiments and simulations, it is confirmed that the ripples can be eliminated and the solidification angles can be decreased by adopting a substrate with lower thermal conductivity. This research provides guidance to achieve good metallurgical bonding and minimizes internal defects in droplet-based 3D printing.

References

[1] D. Zhang, L. Qi, J. Luo, H. Yi, X. Hou, Direct fabrication of unsupported inclined aluminum pillars based on uniform micro droplets deposition, International Journal of Machine Tools and Manufacture, 116 (2017) 18-24.

[2] H. Yi, L. Qi, J. Luo, Y. Jiang, W. Deng, Pinhole formation from liquid metal microdroplets impact on solid surfaces, Applied Physics Letters, 108 (2016) 041601.

[3] T. Zhang, X. Wang, T. Li, Q. Guo, J. Yang, Fabrication of flexible copper-based electronics with high-resolution and high-conductivity on paper via inkjet printing, Journal of Materials Chemistry C, 2 (2014) 286-294.

[4] T. Zhang, M. Hu, Y. Liu, Q. Guo, X. Wang, W. Zhang, W. Lau, J. Yang, A laser printing based approach for printed electronics, Applied Physics Letters, 108 (2016) 103501.

[5] H. Gorter, M. Coenen, M. Slaats, M. Ren, W. Lu, C. Kuijpers, W. Groen, Toward inkjet printing of small molecule organic light emitting diodes, Thin Solid Films, 532 (2013) 11-15.

[6] R. Vellacheri, A. Al-Haddad, H. Zhao, W. Wang, C. Wang, Y. Lei, High performance supercapacitor for efficient energy storage under extreme environmental temperatures, Nano Energy, 8 (2014) 231-237.

[7] C.W. Visser, R. Pohl, C. Sun, G.W. Römer, B. Hu is in't Veld, D. Lohse, Toward 3D printing of pure metals by laser‐induced forward transfer, Advanced materials, 27 (2015) 4087-4092.

[8] M. Fang, S. Chandra, C. Park, Heat transfer during deposition of molten aluminum alloy droplets to build vertical columns, Journal of Heat Transfer, 131 (2009) 112101.

[9] Q. Xu, V. Gupta, E. Lavernia, Thermal behavior during droplet-based deposition, Acta materialia, 48 (2000) 835-849.

[10] W. Liu, G. Wang, E. Matthys, Thermal analysis and measurements for a molten metal drop impacting on a substrate: cooling, solidification and heat transfer coefficient, International Journal of Heat and Mass Transfer, 38 (1995) 1387-1395.

[11] R. Rangel, X. Bian, Metal-droplet deposition model including liquid deformation and substrate remelting, International journal of heat and mass transfer, 40 (1997) 2549-2564.

[12] B. Kang, Z. Zhao, D. Poulikakos, Solidification of liquid metal droplets impacting sequentially on a solid surface, TRANSACTIONS-AMERICAN SOCIETY OF MECHANICAL ENGINEERS JOURNAL OF HEAT TRANSFER, 116 (1994) 436-436.

[13] Y.-p. Chao, L.-h. Qi, H.-s. Zuo, J. Luo, X.-h. Hou, H.-j. Li, Remelting and bonding of deposited aluminum alloy droplets under different droplet and substrate temperatures in metal droplet deposition manufacture, International Journal of Machine Tools and Manufacture, 69 (2013) 38-47.

[14] L.-h. Qi, Y.-p. Chao, J. Luo, J.-m. Zhou, X.-h. Hou, H.-j. Li, A novel selection method of scanning step for fabricating metal components based on micro-droplet deposition manufacture, International Journal of Machine Tools and Manufacture, 56 (2012) 50-58.

[15] S. Schiaffino, A.A. Sonin, Molten droplet deposition and solidification at low Weber numbers, Physics of Fluids, 9 (1997) 3172-3187.

[16] H.-s. Zuo, H.-j. Li, L.-h. Qi, J. Luo, S.-y. Zhong, Y.-f. Wu, Effect of non-isothermal deposition on surface morphology and microstructure of uniform molten aluminum alloy droplets applied to three-dimensional printing, Applied Physics A, 118 (2015) 327-335.

[17] J.M. Waldvogel, D. Poulikakos, Solidification phenomena in picoliter size solder droplet deposition on a composite substrate, International Journal of Heat and Mass Transfer, 40 (1997) 295-309.

[18] J. Waldvogel, D. Poulikakos, D. Wallace, R. Marusak, Transport phenomena in picoliter size solder droplet dispension, Journal of heat transfer, 118 (1996) 148-156.

[19] J. Du, Z. Wei, Z. Chen, S. Li, Y. Tang, Numerical Investigation of Pileup Process in Metal Microdroplet Deposition Manufacture, Micromachines, 5 (2014) 1429-1444.

[20] H. Li, P. Wang, L. Qi, H. Zuo, S. Zhong, X. Hou, 3D numerical simulation of successive deposition of uniform molten Al droplets on a moving substrate and experimental validation, Computational Materials Science, 65 (2012) 291-301.

[21] J. Du, Z. Wei, Numerical analysis of pileup process in metal microdroplet deposition manufacture, International Journal of Thermal Sciences, 96 (2015) 35-44.

[22] R. Ghafouri-Azar, S. Shakeri, S. Chandra, J. Mostaghimi, Interactions between molten metal droplets impinging on a solid surface, International Journal of Heat and Mass Transfer, 46 (2003) 1395-1407.

[23] G.-X. Wang, E. Matthys, Modelling of heat transfer and solidification during splat cooling: Effect of splat thickness and splat/substrate thermal contact, International journal of rapid solidification, 6 (1991) 141-174.

[24] Q. Xu, E. Lavernia, Influence of nucleation and growth phenomena on microstructural evolution during droplet-based deposition, Acta materialia, 49 (2001) 3849-3861.

[25] A. Association, Aluminum: properties and physical metallurgy, ASM International, 1984.

[26] K. Bobzin, N. Bagcivan, D. Parkot, M. Schäfer, I. Petković, Modeling and Simulation of Microstructure Formation for Porosity Prediction in Thermal Barrier Coatings Under Air Plasma Spraying Condition, Journal of Thermal Spray Technology, 18 (2009) 975.

[27] S.D. Aziz, S. Chandra, Impact, recoil and splashing of molten metal droplets, International journal of heat and mass transfer, 43 (2000) 2841-2857.

[28] C. Amon, K. Schmaltz, R. Merz, F. Prinz, Numerical and experimental investigation of interface bonding via substrate remelting of an impinging molten metal droplet, Journal of heat transfer, 118 (1996) 164-172.

[29] V. Mehdi-Nejad, J. Mostaghimi, S. Chandra, Air bubble entrapment under an impacting droplet, Physics of fluids, 15 (2003) 173-183.

[30] J. Stringer, B. Derby, Formation and stability of lines produced by inkjet printing, Langmuir, 26 (2010) 10365-10372.

[31] H. Yi, L. Qi, J. Luo, Y. Guo, S. Li, N. Li, Elimination of droplet rebound off soluble substrate in metal droplet deposition, Materials Letters, 216 (2018) 232-235.

Acknowledgements

The authors gratefully acknowledge the support of the China Scholarship Council, National Natural Science Foundation of China (No. 51675436), Key research and development plan of Shaanxi Province (2017ZDXM-GY-110), Science and Technology fund project, Innovation Foundation for Doctor Dissertation of Northwestern Polytechnical University (No. CX201704).